Magnetic Properties of Mechanically Milled Sm-Co Permanent Magnetic Materials with the TbCu$_7$ Structure

Raphael Justin Joseyphus[1,3], Alwarramanujam Narayanasamy[1,*], Raghavan Gopalan[2], Venkatasubramanian Chandrasekaran[2], Balachandran Jeyadevan[3] and Kazuyuki Tohji[3]

[1]*Materials Science Centre, Department of Nuclear Physics, University of Madras, Guindy Campus, Chennai 600 025, India*
[2]*Defence Metallurgical Research Laboratory, Kanchanbagh, Hyderabad 500 058, India*
[3]*Graduate School of Environmental Studies, Tohoku University, Sendai 980-8579, Japan*

The magnetic properties of Sm(Co,Fe,Cu,Zr)$_7$ compound with the TbCu$_7$ structure are studied for the mechanically milled samples. The coercivity could be varied, without affecting the saturation magnetization, from 44 kA/m for the micron sized particles to 280 kA/m by reducing the particle size to sub-micron size (600–900 nm) using high-energy ball milling. The enhancement in the coercivity is attributed to the particles approaching single domain size. The presence of dipolar coupling suggests that the grain sizes are well above the exchange length for the milled samples. The thermal measurements indicate that the compound with the TbCu$_7$ structure is not stable at high temperatures beyond 743 K.
[doi:10.2320/matertrans.47.2264]

1. Introduction

The Sm-Co permanent magnetic materials have the advantage of possessing higher Curie temperature than that of Nd-Fe-B permanent magnetic materials.[1] They exhibit three structural forms of CaCu$_5$, Th$_2$Zn$_{17}$, and Th$_2$Ni$_{17}$.[2,3] In addition, the TbCu$_7$ structure is also observed, which is a disordered form of CaCu$_5$ structure having P6/mmm space group where one of the Sm atoms is replaced with a transition metal dumbbell pair randomly. The substitution of rare earth atoms by dumbbell pairs in an ordered fashion results in Th$_2$Zn$_{17}$ rhombohedral structure of the type $R\bar{3}m$. The substitution of Fe in Sm-Co system increases the magnetization whereas the Zr or Cu addition helps in the stabilization of the TbCu$_7$ structure and also increases the anisotropy.[4,5] The Sm-Co permanent magnetic materials can be synthesized through mechanical alloying or melt spinning technique.[6,7] However, the synthesis through both the techniques results in the formation of two or more phases,[8–10] which could affect the magnetic properties. A high coercivity of 688 kA/m at a temperature of 773 K has been achieved through proper heat treatments and development of cellular microstructure having Sm$_2$Co$_{17}$ as the main phase and SmCo$_5$ as the grain boundary phase.[11] The coercivity is found to decrease on grain size reduction for the TbCu$_7$ structure of Sm$_2$Co$_{17}$, which is obtained by milling the annealed Sm-Co powder along with Cu as reported by Zhang *et al.*[12] An enhancement in the coercivity and squareness ratio for lower milling durations followed by a gradual deterioration due to amorphisation, on further milling, has been observed in the case of SmCo$_5$ permanent magnetic materials.[3,13] Ball milling SmCo$_5$ with antiferromagnetic powders in an appropriate ratio has resulted in an enhanced coercivity and squareness ratio due to the coupling between both the phases.[14] The increase in coercivity is attributed to various reasons like grain size reduction and pinning of the domain walls by the phases such as SmCo$_5$ and FeZrCu[15]

that segregate at the grain boundary. Since there are already reports on the increase in the coercivity of the Sm-Co compounds by post annealing process, we are interested to study the effect of the magnetic properties of Sm-Co compounds subjected to particle size reduction by milling. In this article, we report on the changes in the magnetic properties on mechanically milling the Sm(Co,Fe,Cu,Zr)$_7$ permanent magnetic material having the TbCu$_7$ structure without any post annealing process. The δM studies were performed to verify whether the particles are isolated or interacting and also the nature of interaction.

2. Experiment

Elements of high purity Sm, Co, Fe, Cu, and Zr were induction melted in the weight percentage of 26, 51, 15, 5, and 3 respectively to form an ingot. The resulting ingot was hand crushed for 5 minutes in an agate mortar in toluene medium. The ball milling was carried out using a high-energy ball mill (Fritsch Pulveresette 7) with agate balls and vial in high purity toluene medium. The ball to powder weight ratio was fixed as 20:1 and the milling speed was 300 rpm. The X-ray diffraction (XRD) measurements were performed using Cu-K$_\alpha$ radiation. The average grain size was estimated using the Scherrer formula. Scanning electron microscopy (SEM) measurements were performed to study the morphology of the samples. Magnetic measurements at 300 K were performed using a vibrating sample magnetometer (VSM) with a maximum applied field of 2 T by fixing the samples in wax. Thermomagnetization (TM) measurements were performed in Ar atmosphere using a Perkin Elmer thermogravimetric analyzer (TGA) and a small horse shoe magnet with a field strength of 4 mT.

3. Results and Discussions

3.1 Structure, grain size, and morphology

Figure 1 shows the XRD of the Sm(Co,Fe,Cu,Zr)$_7$ compound for various milling durations. The XRD is indexed

---

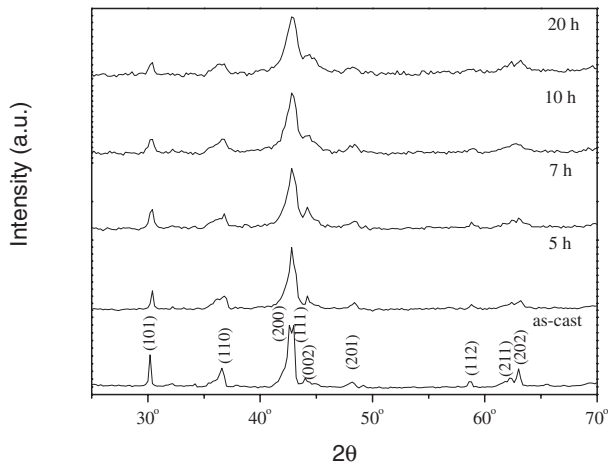*Corresponding author, E-mail: ansuom@yahoo.co.in

Fig. 1 The XRD of the Sm(Co,Fe,Cu,Zr)₇ compound with the TbCu₇ structure milled for various durations.

Fig. 2 The average grain size for the Sm(Co,Fe,Cu,Zr)₇ compound milled for various durations.

corresponding to the hexagonal P6/mmm phase with the TbCu₇ structure. The absence of the (015) peak of the Th₂Zn₁₇ structure between (110) and (200) reflections suggests that the Th₂Zn₁₇ structure is not present in the samples. The lattice parameters calculated from the XRD peak positions are $a = 0.4903$ nm and $c = 0.4109$ nm. The c/a ratio is 0.84 which is in agreement with the reported value for the TbCu₇ hexagonal structure[16] with a unit cell volume of 0.08554 nm³. The grain size decreases on milling as seen from the line broadening of the XRD peaks. The shoulder near the (110) peak occurs probably due to the disordered nature of TbCu₇ phase.[17] On milling, the (200)

and (111) peaks merge into a single peak. The average grain size calculated, using the Scherrer formula, from the width of the (101) peak is found to decrease from 72 nm in the as prepared state (bulk) to 15 nm for the 20 h milled sample as shown in Fig. 2. Although correction for strain is not incorporated in the XRD line broadening, the magnetic properties are correlated to the particle sizes determined from SEM measurements.

Figure 3 shows the SEM micrographs of the as-cast, 10 h milled and 20 h milled Sm(Co,Fe,Cu,Zr)₇ samples. The as-cast samples have micron-sized particles as seen from the SEM picture. On milling to 10 h, the particles become submicron in size around 600–900 nm and also some particles are found to be slightly agglomerated. The repeated

Fig. 3 The SEM pictures of the (a) as-cast, (b) 10 h milled, and (c) 20 h milled Sm(Co,Fe,Cu,Zr)₇ compound.

Fig. 4　The hysteresis loop at 300 K for the (a) as-cast, (b) 10 h and (c) 20 h milled Sm(Co,Fe,Cu,Zr)$_7$ compound.

Fig. 5　The coercivity and remanence ratio of the Sm(Co,Fe,Cu,Zr)$_7$ compound milled for various durations.

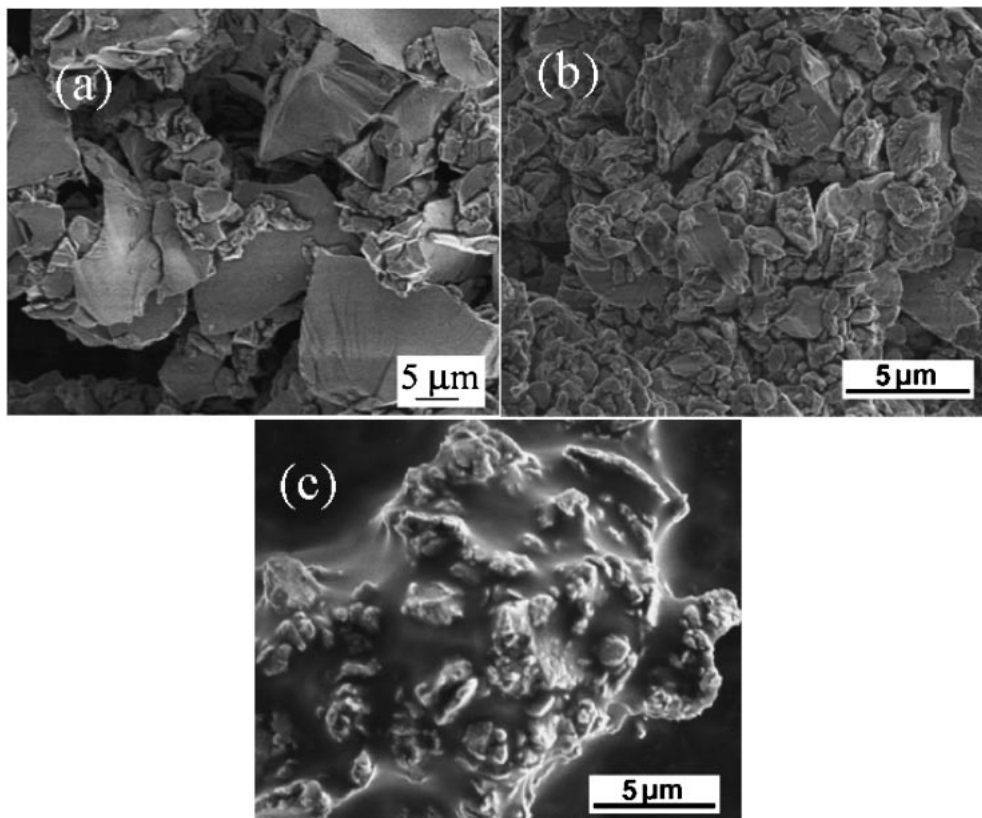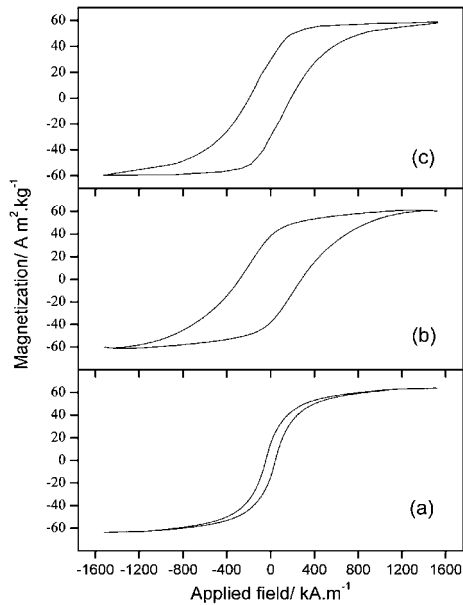breaking and welding of the particles leads to a change in the particle size and morphology. As milling introduces highly irregular particle sizes and shapes, the average particle size is estimated from the most probable distribution in the sizes. This could be visualized from the comparatively larger particle size for the as-cast samples which decreases with milling although a small number of particles with bigger and smaller sizes are being found in all the three samples. When milled for 20 h, the small particles are welded together to form agglomerates as visible from the SEM pictures.

3.2　Magnetic Properties

Figures 4(a), (b) and (c) show the hysteresis loops of the as-cast, 10 and 20 h milled Sm(Co,Fe,Cu,Zr)$_7$ samples respectively at 300 K. The coercivity of the samples increases on milling whereas the saturation magnetization remains almost constant at 60 Am^2/kg up to 20 h milling. The smooth hysteresis loop is indicative of the presence of a single phase only; otherwise, the presence of two or more magnetic phases would result in a kink in the hysteresis loop in the absence of exchange coupling. Figure 5 shows the coercivity and remanence ratio for the Sm(Co,Fe,Cu,Zr)$_7$ powders for various milling times. The coercivity increases with milling from 44 kA/m for the as-cast to 280 kA/m for 10 h of milling and then decreases to 200 kA/m on further milling to 20 h. The coercivity for the ball-milled SmCo$_{6.7}$Cu$_{0.3}$ alloy with the TbCu$_7$ structure is reported to be 80 kA/m which increases with the formation of Th$_2$Zn$_{17}$ structure on annealing.[18] The melt-spun ribbons of Sm(Co$_{0.85}$Fe$_{0.15}$)$_{7.6}$ with the TbCu$_7$ structure have shown a higher coercivity of 212 kA/m with grain size reduction to 5–0.5 μm[8] whereas for the SmCo$_{6.4}$Zr$_{0.4}$ melt-spun ribbon with the same structure, the coercivity is only 144 kA/m, because of the texture effects.[19] The composition Sm(Co$_{0.85}$Fe$_{0.15}$)$_{7.6}$ is expected to show a lower coercivity due to the reduced anisotropy, because of the substitution of Fe, compared to
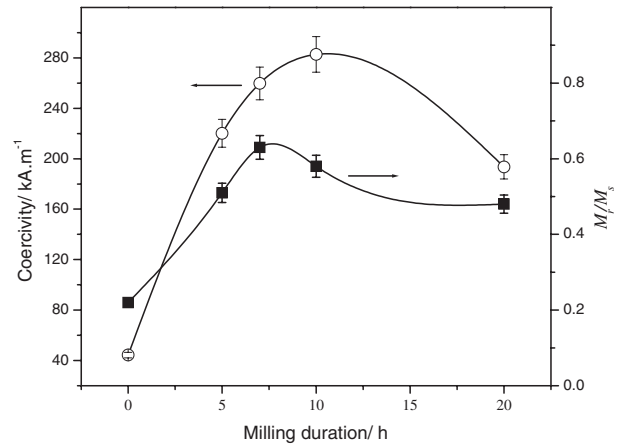
SmCo$_{6.4}$Zr$_{0.4}$ with the same TbCu$_7$ structure. Chen *et al.*[20] showed an increase in the coercivity for the Sm$_2$Co$_{17}$ compound due to grain size reduction with a maximum value of 320 kA/m after milling for 20 min and a decrease with milling for higher duration due to the formation of amorphous phase. From the earlier reports in the literature we understand that the estimation of grain size-dependent coercivity in melt-spun ribbons is made difficult by the texture effects and that the amorphization in the ball milled samples decreases the coercivity. The increase of coercivity in the present study is believed to be due to particle size reduction. The TbCu$_7$ structure remains stable with milling and the XRD is not able to detect any weak impurity phases, if present, due to the smaller grain size and disorder induced by ball milling. However, the magnetic properties are not found to deteriorate with milling and almost the same value for the magnetization is obtained even after milling. Even though the values of coercivity obtained in the present study are less than the values reported for the heat treated samples,[11] they are still quite significant and also we could increase the coercivity from a low value of 44 to 280 kA/m by ball milling and without using any heat treatment. The increase in coercivity with milling is due to the particle size reduction leading to the single domain state. The milling of the particles in the toluene medium, compared to the samples milled in an inert atmosphere, has facilitated the formation of less agglomerated particles on milling up to 10 h resulting in an increase in coercivity. The critical diameter D_c of the single domain particles can be estimated using the relation[21]

$$D_c = C_o \frac{\sqrt{AK_1}}{\mu_o M_s^2} \qquad (1)$$

where $C_o = 72$, A is the exchange constant which is of the order of 10 pJ/m, K_1 is the magnetic anisotropy constant, and M_s is the saturation magnetization. By substituting the values of K_1 calculated from the anisotropy field reported in the literature for the SmCo$_{7-x}$Zr$_x$ compound with the same TbCu$_7$ structure[22] in eq. (1), the critical single domain size is calculated to be around 706 nm for the compound in the present study, assuming that the particles are spherical in shape, and also subject to a small error that may arise due to a

slight difference in the K_1 values of the two compositions. Since the high-energy ball milling would result in non-spherical shape for the particles, the actual critical size of the single domain particle should be larger as the elongated particles have a lower demagnetization factor.[23] Since the calculated single domain size is near the experimentally observed particle size of nearly 600–900 nm as seen from Fig. 3, the increase in the coercivity with milling up to 10 h is due to the particles approaching the single domain size. However, the coercivity decreases for milling beyond 10 h due to agglomeration of the particles, which is evident from the scanning electron micrograph.

According to the Stoner-Wohlfarth relation, non-interacting isolated particles have a remanence ratio below 0.5. But in the present study, the remanence ratio increases with milling and becomes greater than 0.5 after 5 h of milling. The enhanced remanence ratio suggests the presence of exchange or dipolar interaction between particles.[24,25] In order to verify the nature of interactions, δM studies were performed at 300 K for the milled samples. The δM values are calculated from the Isothermal Remanence Magnetization (IRM) measurements, which is done by plotting the remanent magnetization as a function of field from a demagnetized sample and from the Direct Current Demagnetization (DCD) measurements by applying a reverse field and measuring the demagnetization curve of the sample. From these measurements the parameter δM, which is defined as[26]

$$\delta M = \frac{\{M_D(H) - [M_r(H_{\max}) - 2M_R(H)]\}}{M_r(H_{\max})} \quad (2)$$

where $M_D(H)$ is the DCD remanence, $M_R(H)$ is the IRM, and $M_r(H_{\max})$ is the saturation remanence, is plotted against the applied field H. A positive value for δM represents exchange interaction and a negative value represents dipolar interaction between the grains whereas a zero value is obtained for non-interacting particles with uniform pinning of domain walls.[27]

Figure 6 shows the variation of δM at 300 K with applied field for various milling durations for Sm(Co,Fe,Cu,Zr)₇. The nonzero value for δM suggests that there is no uniform pinning of domain walls and the negative value for all the samples confirms the presence of dipolar interactions. The dipolar coupling decreases with particle size reduction on milling from 5 to 7 h as could be seen from the decrease in the peak height. With further increase in the milling duration to 10 h the area of the δM peak increases. The nonuniformity of particle sizes, which is inherent in the milled samples, results in a large distribution in dipolar interactions for the 10 h milled samples. The δM peak intensity decreases with milling up to 10 h indicating that the strength of the dipolar interaction decreases with particles size reduction. However, the dipolar interaction strength is observed to increase on further milling to 20 h, which might be due to the stray fields[28,29] originating from defects and non-ideal grain boundaries introduced by milling which prevents the exchange interaction. The dipolar interaction strength also depends on the positional disorder present in the system.[30] The change in the morphology of the particles due to agglomeration, defects and microstructural changes introduced by milling may also have resulted in the decrease in the remanence ratio and enhanced dipolar interaction overcom-
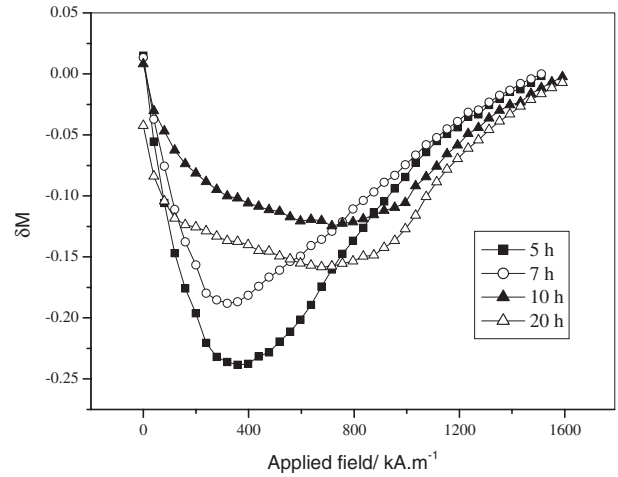
Fig. 6   The δM curves at 300 K for the Sm(Co,Fe,Cu,Zr)₇ compound milled for various durations.

ing exchange interaction. The exchange interaction is found to depend on the exchange length which is only a few nm and hence much smaller compared to the single domain size which is of the order of a few hundred nanometer in Sm-Co type of permanent magnets.[21] From the δM studies we could understand that the grain sizes are well above the exchange length since there is only dipolar interaction.

In Sm-Co permanent magnetic materials, large coercivities are achieved by developing cellular microstructure in the Sm₂Co₁₇ phase where the domain walls are pinned by the SmCo₅ phase which acts as pinning centers.[2] The cellular microstructure develops only with complex heat treatment procedures. In order to develop the suitable microstructure by heat treatment we have carried out thermomagnetic measurements to check the thermal stability of the present compound with the TbCu₇ structure. Figure 7 shows the thermomagnetization measurement, using TGA with a small applied field, for the as-cast Sm(Co,Fe,Cu,Zr)₇ compound up to 923 K. The as-cast alloy shows an increase in the weight above 743 K denoted by T_{cr} as shown in the TGA curve (Fig. 7) which may be due to the crystallization of another phase. The weight gain indicates that the crystallized phase is magnetic. The XRD, shown in the inset of Fig. 7, reveals that the crystallized phase is the ordered Th₂Zn₁₇ structure which is responsible for the observed increase in the weight in the thermomagnetization measurement beyond 743 K due to its higher magnetization value than that of the TbCu₇ structure. The magnetic measurements for the sample milled for 10 h and subsequently annealed at 873 K show that the coercivity drops to less than 48 kA/m from 280 kA/m. The instability of the phase also makes it difficult to find the Curie temperature of the samples.

4. Conclusions

The coercivity of the Sm(Co,Fe,Cu,Zr)₇ compound was varied from 44 kA/m for the bulk to 280 kA/m by controlling the particle size using high-energy ball milling without affecting the saturation magnetization. Interestingly, a high coercivity could be obtained in mechanically milled powders

Fig. 7 The thermomagnetic measurement using TGA for the as-cast Sm(Co,Fe,Cu,Zr)$_7$ compound. Inset shows the XRD of the as-cast Sm(Co,Fe,Cu,Zr)$_7$ compound annealed at 873 K with the Th$_2$Zn$_{17}$ structure.

without subjecting them to any post annealing step. The increase in the coercivity is attributed to the particles approaching single domain size. The particles showed dipolar coupling which is found to decrease with milling up to 10 h suggesting that the grain sizes are well above the exchange length. The thermal measurements show that the compound is not stable above 743 K.

Acknowledgements

REFERENCES

1) J. F. Liu, T. Chui, D. Dimitrov and G. C. Hadjipanayis: Appl. Phys. Lett. **73** (1998) 3007–3009.
2) K. H. J. Buschow: *Handbook of Magnetic Materials*, Vol. 10, (Elsevier, Amsterdam, 1997).
3) K. Kumar: J. Appl. Phys. **63** (1988) R13–R57.
4) I. A. Al-Omari, J. Zhou and D. J. Sellmyer: J. Alloys and Compds. **298** (2000) 295–298.
5) M. Q. Huang, M. Drennan, W. E. Wallace, M. E. McHenry, Q. Chen and B. M. Ma: J. Appl. Phys. **85** (1999) 5663–5665.
6) P. A. I. Smith, J. Ding, R. Street and P. G. McCormick: Scripta Mater. **34** (1996) 61–66.
7) A. Yan, A. Bollero, K.-H. Müller and O. Gutfleisch: Appl. Phys. Lett. **80** (2002) 1243–1245.
8) C. H. Chen, S. Kodat, M. H. Walmer, S.-F. Cheng, M. A. Willard and V. G. Harris: J. Appl. Phys. **93** (2003) 7966–7968.
9) V. G. Harris, M. Liou, B. N. Das, V. M. Browning, J. E. Snyder, M. Rubinstein, S. H. Lawrence, R. Littleton III and D. P. Pappas: J. Appl. Phys. **81** (1997) 5121–5123.
10) J. E. Shield and B. E. Meacham: J. Appl. Phy. **87** (2000) 2055–2057.
11) J. Zhou, R. Skomski, C. Chen, G. C. Hadjipanayis and D. J. Sellmyer: Appl. Phys. Lett. **77** (2000) 1514–1516.
12) J. X. Zhang, L. Bessais, C. Djega-Mariadassou, E. Leroy, A. Percheron-Guegan and Y. Champion: Appl. Phy. Lett. **80** (2002) 1960–1962.
13) D. L. Leslie-Pelecky and R. L. Schalek: Phys. Rev. B **59** (1999) 457–462.
14) J. Sort, S. Surinach, J. S. Munoz, M. D. Baro, J. Nogues, G. Chouteau, V. Skumryev and G. C. Hadjipanayis: Phys. Rev. B **65** (2002) 174420.
15) G. C. Hadjipanayis: J. Appl. Phys. **55** (1984) 2091–2093.
16) K. H. J. Buschow and A. S. Van der Goot: Acta Cryst. B **27** (1971) 1085–1088.
17) F. J. Cadieu, H. Hegde, N. Kamprath, A. Navarathna and R. Rani: *Proc. Eleventh Int. Workshop on Rare Earth Magnets and their Applications*, Pennsylvania, Vol. II (1990) 463.
18) M. Venkatesan, C. Jiang and J. M. D. Coey: J. Magn. Magn. Mater. **242–245** (2002) 1350–1352.
19) A. R. Yan, Z. G. Sun. W. Y. Zhang, H. W. Zhang and B. G. Shen: Appl. Phys. A **71** (2000) 311–314.
20) Z. Chen, X. Meng-Burany, H. Okumura and G. C. Hadjipanayis: J. Appl. Phys. **87** (2000) 3409–3414.
21) R. Skomski: J. Phys. Condens. Mater. **15** (2003) R841–R896.
22) M. Q. Huang, W. E. Wallace, M. McHenry, Q. Chen and B. M. Ma: J. Appl. Phys. **83** (1998) 6718–6720.
23) B. D. Cullity: *Introduction to Magnetic Materials* (Addison-Wesley Publishing Co., Massachusetts, 1972).
24) Q. Chen, B. M. Ma, B. Lu, Q. Huan and D. E. Laughlin: J. Appl. Phys. **85** (1999) 5917–5919.
25) H. Ku and J. Y. Li: Phys. Rev. B **68** (2003) 212402.
26) P. E. Kelly, K. O'Grady, P. I. Mayo and R. W. Chantrell: IEEE Trans. Magn. **25** (1989) 3880–3883.
27) G. C. Hadjipanayis and A. Kim: J. Appl. Phys. **63** (1988) 3310–3315.
28) R. Fisher and H. Kronmüller: J. Appl. Phys. **83** (1998) 3271–3275.
29) V. Neu, A. Hubert and L. Schultz: J. Magn. Magn. Mater. **189** (1998) 391–396.
30) M. Porto: J. Appl. Phys. **92** (2002) 6057–6061.